

A COMPARATIVE STUDY OF (ZnO, In₂O₃:SnO₂, SnO₂)/CdS/CdTe/(Cu)/Ni HETEROJUNCTIONS

Sergiu Vataavu¹, Corneliu Rotaru¹, Vladimir Fedorov¹, Timo A. Stein², Mihail
Caraman¹, Igor Evtodiev¹, Carola Kelch², Michael Kirsch²,
Petru Chetruș¹, Petru Gașin¹, Martha Ch. Lux-Steiner² and Marin Rusu^{1,2}

¹*Faculty of Physics and Engineering, Moldova State University, 60 A. Mateevici str.,
MD-2009 Chisinau, Republic of Moldova*

²*Institut für Heterogene Materialsysteme, Helmholtz-Zentrum Berlin für Materialien
und Energie, Lise-Meitner-Campus, Hahn-Meitner-Platz 1, 14109 Berlin, Germany*

Abstract

The influence of the manufacturing technology on the structural properties of CdTe and CdS layers, components of the CdS/CdTe solar cells has been investigated. CdTe based solar cells have been prepared using glass substrates coated with different transparent conductive oxides (TCOs: SnO₂, In₂O₃:SnO₂ (ITO), ZnO:Al, ZnO:Al/i-ZnO).

The analysis of the technology combined with various investigation methods allowed to determine optimum deposition parameters for CdS and CdTe for each type of TCO used. X-ray diffraction (XRD) and grazing incidence XRD analysis have been carried out for TCO, CdS, and CdTe layers at different deposition stages before and after annealing in the presence of CdCl₂ in air. The reflection spectra in the 100-600 cm⁻¹ spectral region have been thoroughly studied by using Fourier transform infrared spectroscopy. It was found that (i) the best quality possess CdS and CdTe thin films

sequentially deposited on ZnO:Al substrates and that (ii) the pre-treatment defects can be effectively cured and most of the secondary phases can be removed by annealing, while the basic structure of the investigated thin films does not essentially change.

Keywords

CdS, CdTe, heterojunction, CSS, CBD, HWT, XRD, FTIR

1. Introduction

CdTe is a material extensively studied at micro and nanoscale due to the possibility of its use in ionizing radiation detectors and in photovoltaic (PV) applications [1, 2]. The mostly studied PV application for CdTe is related to its use in CdS/CdTe heterojunction solar cell. Thin film solar cells are still having a serious development problem, considering that the efficiency increase progresses are barely being noticed. The record efficiency value remaining at 16.5% [3] despite the fact a large number of investigations in different groups resulted in a thorough physical and chemical analysis of the devices. Technological variations resulting in structural modifications of thin films and changes in physical processes might lead to progresses. The quality of thin semiconductor films and devices based on them are highly influenced by the deposition technology [4, 5].

This paper is focused on structural analysis of CdS thin films deposited by chemical bath deposition (CBD) and close spaced sublimation (CSS) on different transparent conductive oxides (TCOs). Furthermore analysis of CdTe thin films is carried out on CSS and hot wall technique (HWT) obtained samples deposited onto CdS/TCO/Glass substrate. The influence of CdTe annealing in presence of CdCl₂ is studied by investigating the x-ray diffraction (XRD) patterns. In the 100-600 cm⁻¹ region the vibrational spectra of CdTe films in device configuration is studied.

2. Experimental details

Glass coated with different types of TCOs has been used as a substrate. The Präzisions Glas & Optik GmbH 5 Ω /square Indium Tin Oxide (ITO), approx. 310 nm thick, SiO₂ of approx. 25 nm thick and Glass constituted the ITO substrates. Commercially available Glass covered with SnO₂ (transparency ~80% in the visible spectral region) has been used as alternative substrates. Another types of front contacts used in our experiments were ZnO:Al and *i*-ZnO/ZnO:Al bilayer. The sputtered layer consists of a 90-nm intrinsic and a 400-nm highly Al-doped ZnO. The optical transmission in the visible spectral region was ~82-84% for the ZnO:Al.

CdS window layer has been deposited by: CBD, CSS and HWT deposition. The CBD-CdS layer with the thicknesses from 40 nm to 80 nm have been prepared by using standard chemical bath deposition from solution of ammonia (NH₃) and thiourea (H₂NCSNH₂) at 60°C [6].

CdS thin films have been deposited by a modified CSS system using the deposition chamber sketched in Fig. 1a. The germination and layer's initial formation conditions have been changed by choosing the appropriate temperature for the substrate and source (for all TCOs used SnO₂, ITO, ZnO:Al, *i*-ZnO/ZnO:Al). The substrate temperature, T_{sub} , was varied in the range of 270-465°C. The source temperature, T_{source} , was varied from 545°C to 650°C. The decrease of deposition rate was possible by introducing a grating G (Fig. 1a). The CdS film thickness was measured as 0.1-0.7 μm . The temperature dependence of the electrical conductivity indicates an activation character in the temperature range of 295-415K. The activation energy determined from this dependence equals to ~0.44 eV. The concentration of charge carriers determined from Hall measurements was $4\text{-}6\cdot 10^{17} \text{ cm}^{-3}$ (294K).

Also, CdS thin films have been deposited in a HWT deposition chamber, of which a sketch is given in Fig. 1b. The substrate temperature during deposition was of 330-420°C. The temperature in the T₃ zone of the deposition chamber was 525-565°C. The layer thicknesses are in the same range as for the CSS-CdS.

The next technological step in the solar cell fabrication consists in CdTe absorber deposition by CSS or HWT using an apparatus similar to the one described in Figs. 1a and 1b. The deposition temperature for the CSS CdTe was 500-550°C, while the substrate temperature being 340-450°C. The deposition temperature range for the CdTe deposited by HWT system was the same as for CSS CdTe. In both cases the thickness of the layers was 5-6 μm.

Annealing in the presence of CdCl₂ (in air) of the Glass/TCO/CdS/CdTe structure at 385-410°C for 25 min and its etching in Br-methanol solution were carried out. Cu (4 nm)/Ni (120 nm) bi-layer has been used as back contact for CdTe.

The analysis of a large series of samples (approx. 20 for each TCO) allowed to establish that for deposition apparatus and materials used, the application of the CSS method lead to slightly better (cca. 2-3%) PV parameters (such as short-circuit current (J_{sc}), open circuit voltage (V_{oc}), fill factor (FF) and efficiency (η)) when compared to those of the HWT prepared solar cells. Hence, the following analysis will give consideration to samples obtained by CSS only. One can underline the optimum deposition temperatures for CdS deposited by CSS onto TCO/Glass substrates as:

(i) TCO=ITO: T_{sub}=460-465°C, T_{source}=650°C;

(ii) TCO=ZnO:Al: T_{sub}=415°C, T_{source}=550°C;

(iii) TCO=*i*-ZnO/ZnO:Al: T_{sub}=320°C, T_{source}=535-540°C;

(iv) TCO=SnO₂: T_{sub}=415-420°C, T_{source}=650°C.

The sublimation of CdTe thin films is optimum in the following conditions: $T_{\text{sub}}=465^{\circ}\text{C}$ and $T_{\text{source}}=555^{\circ}\text{C}$.

The XRD analysis and grazing incidence XRD (GI-XRD) measurements have been carried out by using of Bruker D8 Advance. FullProf Suite 2011 and BRUKER EVA software has been used for XRD analysis. A Jasco 6300 spectrometer was used for Fourier transform infrared (FTIR) spectroscopy. The scanning electron microscopy (SEM) has been performed with a Gemini Leo 1530 system.

3. Results & discussion

The typical obtained sample's cross section by SEM is given in Fig. 2a. One can notice the structure of the surface of (unannealed) CdTe film in Fig. 2b. X-ray diffraction patterns for CdS and CdTe are well known [7, 8]. The main analysis should be focused on CdS thin films deposited onto real device substrate (i.e. ZnO:Al/Glass etc.) due to the fact that the substrate strongly affects the morphology and other properties of the next layer to be deposited (CdTe).

3.1 CdS XRD The GI-XRD pattern of CdS thin films deposited by CBD and CSS on various substrates is given in Fig. 3. One can see that the diffractogram for the CBD-CdS (1) reveals a large number of diffraction peaks which are assigned to substrate (ITO) and the CdS layer which indicate the presence of the cubic phase of CdS (F43 m, AMCSD #18121). This feature was common for all CBD-CdS samples. The cubic phase in CdS is usually observed in as grown layer by CBD [6, 9] and a transition to hexagonal phase may occur after annealing. The first observed peak for c-CdS is positioned at 26.89° being a relatively wide ($\sim 2.2^{\circ}$). The analysis of the texture coefficients P_{hkl} (see Table 1) according to Ref. 10 indicated that the preferred orientation for CBD-CdS growth is the [111] plane.

CdS deposited onto ITO by using CSS and HWT system gave XRD patterns similar to the ones given in Fig. 3 (curve 2). The plot has distinctive peaks attributed both to In_2O_3 (IC 13, AMCSD #17469) and CdS. The ITO pattern is well fitted by In_2O_3 phase only. However, the CdS phase is present as hexagonal phase (h-CdS, P63 mc, AMCSD #15177) for CSS-CdS. The comparison of the CSS and CBD deposited CdS samples shows that the first one has much better crystallinity and quality (at higher fabrication temperature) with the (002) peak at (26.52°) (h-CdS) being predominant.

The change of substrate from ITO to ZnO:Al and i-ZnO/ZnO:Al causes visible modifications of the XRD pattern (Fig. 3 curves 3 and 4). Resulting from modeling and calculations shown in Table 2, the preferred orientation of the h-CdS crystallites is [002]. Only hexagonal phase of CdS has been detected in this configuration (CSS). It has been observed that the lattice parameters for ZnO are slightly changed due to the presence of Al atoms ($a=3.24898 \text{ \AA}$ $c=5.2081 \text{ \AA}$ for ZnO:Al; $a=3.25213 \text{ \AA}$ $c=5.20547 \text{ \AA}$ for i-ZnO substrates). A comparative review of structural parameters for CdS films deposited onto different substrates is given in Table 3. The estimated grain size for CSS CdS is approx. 4-5 times larger than of CBD CdS and the structural quality of CSS CdS films is much better (the suggestion on the quality of CdS films is confirmed by low temperature photoluminescence (PL) experiments, unpublished results). The obtained results are consistent with the published ones in Ref. 11.

3.2 CdTe XRD The CdTe layers XRD patterns have been analyzed for the absorber deposited on $\text{CdS}_{\text{CSS}}/\text{ITO}$, $\text{CdS}_{\text{CSS}}/\text{ZnO:Al}$, $\text{CdS}_{\text{CSS}}/\text{i-ZnO/ZnO:Al}$ as well as for $\text{CdS}_{\text{CSS}}/\text{SnO}_2$ substrates (in the same technological conditions) reported above with exception of the $\text{CdS}_{\text{CBD}}/\text{ITO}$ substrates for annealed and unannealed samples, a few examples of these are given below. The XRD pattern for CdTe thin films deposited on different substrates is shown in Fig. 4. Only the cubic CdTe phase is found, and all samples had a preferential growth of the (111) plane (peak at $2\Theta=23.71^\circ$) (a supportive

example is given in Table 4). Although advanced fitting was carried out, there are still several peaks, unidentified (at $2\Theta=36.04^\circ$, 67.75° , 37.81° , 21.45° , 36.44°). One can only presume that these peaks might be caused by $\text{CdS}_x\text{Te}_{1-x}$ interface layer, or even an oxygen containing phase. Presence of CdO , or CdTeO_3 has been confirmed in Ref. 12. The XRD plot (Fig. 4) shows the presence of h-CdS peaks, and for each substrate, low intensity peaks generated by TCO have also been found.

The influence of the substrate temperature during CdS deposition on the structure of CdTe has been investigated (XRD pattern not shown). It has been established, that in the XRD diffractograms of CdTe, the decrease of the substrate temperature from 440°C to 265°C , causes the intensity decrease of the (002) h-CdS peak; while its broadening for both unannealed and annealed samples, suggests reduced quality of CdS films. Our XRD data is consistent with other publications [13] except of the presence of (200) CdTe peak.

The annealing in CdCl_2 does not modify the shape and pattern of the diffractogram significantly (Fig. 5). After annealing the 36.44° peak vanishes while the other peaks are still present in Figs. 4 and 5, their nature being unknown at the moment. The lattice constant and interplanar distance (d_{111}) remains constant regardless of substrate and annealing ($a=6.4946 \text{ \AA}$, $d_{111}=3.7496 \text{ \AA}$; $a=6.4944 \text{ \AA}$ for CdTe deposited onto CdS/ITO only) (to underline that CdTe is deposited in the same technological regime). The d_{111} value determined in this work (CdTe deposited in vacuum) is lower than for oxygen containing CdTe [14].

The thermal annealing's influence on the XRD patterns of CdTe deposited by HWT is much more evident than in case of CSS-CdTe. As one can see in Fig. 6, there is still an unidentified peak (45.25°) but as a result of treatment it disappears and the XRD peaks became sharp with a well-defined base. Thus, one can assume that some structural defects are cured, and the structure is improved.

3.2.1 CdTe FTIR analysis The spectrum of lattice vibration might give information on the quality and impurities inside the film. The CdTe thin films reflection spectrum in the 100-600 cm^{-1} spectral region is given in Fig. 7. The minimum determined by TO CdTe lattice vibrations can be clearly seen at wave number value of 154.5 cm^{-1} . Its shift relative to reported values of ω_{TO} [15] can be explained by the existence of lattice vibrations related to the lattice defects in CdTe (strain etc). The frequency of LO vibrations are in good agreement with the theoretically calculated values [15]. It has been observed that the band in the wave number interval of 300-500 cm^{-1} contains minima, which can be associated with cadmium and tellurium vacancies defects, alike for example in the hydrogenated CdTe [16].

4. Conclusions

A comparative analysis of XRD patterns obtained for CdS deposited onto different substrates has been carried out. The influence of substrate and annealing for CdTe thin films on XRD patterns is demonstrated. Particularly, it has been observed that for low T_{sub} of CdS deposition on i-ZnO/ZnO:Al substrate, secondary phases related to defects (impurities) have been found. After annealing these phases vanish. The best CdTe quality has been obtained for the layers deposited on CdS layers grown at higher substrate temperatures. A slightly improved CdS quality is obtained on ZnO:Al substrates.

No major structural changes have been found after annealing in the presence of CdCl_2 , but some pre-treatment impurities (or defects) were cured (CSS CdTe). The nature of some peaks remained unknown and should be further investigated. HWT-CdTe layers show the presence of unknown phases in the XRD data which vanish after annealing and thus indicating an improved quality of the films.

As-deposited CdTe thin films show FTIR reflection spectra with minima caused by vibrations due to a large number of defects.

Acknowledgements

This work was supported by Bilateral Moldova-Germany ASM/BMBF grant MDA 09/023 and 10.820.05.03GA and institutional grant 11.817.05.12A. S.V. would like to acknowledge the rectorate of the Moldova State University and the Policontract SRL company (Republic of Moldova) for substantially supporting first author's participation at EMRS Spring Meeting 2012 Symposium B. ICSD structural data has been kindly provided by Dr. Michael Tovar (Helmholtz-Zentrum Berlin) confirming the AMCSD values.

References

- [1] K. Okada, H. Yasufuku, H. Yoshikawa, Y. Sakurai, Appl. Phys. Lett. 92 (2008) 073501.
- [2] J. Britt, C. Ferekides, Appl. Phys. Lett. 62 (1993) 2851.
- [3] X. Wu, J.C. Keane, R.G. Dhere, C. DeHart, D.S. Albin, A. Duda, T.A. Gessert, S. Asher, D.H. Levi, P. Sheldon, 17th European Photovoltaic Solar Energy Conference, Munich, Germany, 22-26 October 2001, Proceedings, (2001) 995.
- [4] T. Okamoto, H. Harada, A. Yamada, M. Konagai, Sol. Energy Mater. & Sol. Cells 67 (2001) 187.
- [5] Junfeng Han, C. Spanheimer, G. Haindl, Ganhua Fu, V. Krishnakumar, J. Schaffner, Chunjie Fan, Kui Zhao, A. Klein, W. Jaegermann, Sol. Energy Mater. & Sol. Cells 95 (2011) 816.
- [6] M. Rusu, A. Rumberg, S. Schuler, S. Nishiwaki, R. Würz, M. Dzierdzina, C. Kelch, S. Siebentritt, R. Klenk, Th. Schedel-Niedrig, M.Ch. Lux-Steiner, J. Phys. and Chem. of Solids 64 (2003) 1849.
- [7] American Mineralogist Crystal Structure Database (AMCSD):
<http://rruff.geo.arizona.edu/AMS/amcsd.php>
- [8] T. Toyama, K. Matsune, H. Oda, M. Ohta, H. Okamoto, J. Phys. D: Appl. Phys. 39 (2006) 1537.
- [9] R. Ramirez-Bon, N.C. Sandoval-Inda, F. J. Espinosa-Beltran, M. Sotelo-Lerma, O. Zelaya-Angel, C. Falcony, J. Phys.: Condens. Matter 9 (1997) 10051.
- [10] G. Zoppi, K. Durose, S. J. C. Irvine, V. Barrioz, Semicond. Sci. Technol. 21 (2006) 763.
- [11] H. R. Moutinho, D. Albin, Y. Yan, R. G. Dhere, X. Li, C. Perkins, C.-S. Jiang, B. To, M. M. Al-Jassim, Thin Solid Films 436 (2003) 175.

- [12] B. E. McCandless, S. S. Hegedus, R. W. Birkmire, D. Cunningham, *Thin Solid Films* 431-432 (2003) 249.
- [13] J. D. Major, Y. Y. Proskuryakov, K. Durose, G. Zoppi, I. Forbes, *Sol. Energy Mater. & Sol. Cells* 94 (2010) 1107.
- [14] H. Arizpe-Chavez, F. J. Esponzoza-Beltran, R. Ramirez-Bon, O. Zelaya-Angel, J. Gonzalez-Hernandez, *Solid State Commun.* 101 (1997) 39.
- [15] E. Degl'ioz, K. Colakoglu, Y. Ciftci, *Physica B* 373 (2006) 124.
- [16] Mao-Hua Du, Hiroyuki Takenaka, David Singh, *J. Appl. Phys.* 104 (2008) 093521.

Figure captions

Figure 1 Sketches of (a) the modified CSS system and (b) the HWT deposition system used for the preparation of CdS and CdTe thin films at Moldova State University

E – CdS (CdTe) source chamber (graphite);

P – substrate (glass or mica);

SP – tube for sample positioning (quartz);

G – grating;

M – source material;

S – substrate heater block (graphite);

SW – heater spiral (tungsten).

T₁, T₂, T₃ – thermocouple (1st wire Ni-90%+Cr-10%, 2nd wire Ni-95%+Mn-3%+Al-2%+Si-1%);

SH – thermal shield (steel)

CT – quartz tube for heater spiral positioning

Figure 2 SEM cross-section view of typical Glass/ZnO:Al/CdS/CdTe/Ni structure (a) and image of the CdTe surface of such unannealed structure (b).

Figure 3 The XRD patterns for CdS thin films deposited by using CBD and CSS methods onto (1) CBD CdS – ITO, (2) CSS CdS – ITO, (3) CSS CdS – ZnO:Al and (4) CSS CdS – i-ZnO/ZnO:Al substrates.

Figure 4 The XRD diffractograms for CdTe thin films deposited by CSS onto (1) CdTe/CdS/ZnO:Al, (2) CdTe/CdS/SnO₂, (3) CdTe/CdS/i-ZnO/ZnO:Al and (4) CdTe/CdS/ITO substrates (unannealed heterojunctions).

Figure 5 The XRD patterns for CdTe thin films deposited by CSS onto (1) CdTe/CdS/ZnO:Al, (2) CdTe/CdS/SnO₂, (3) CdTe/CdS/i-ZnO/ZnO:Al and (4) CdTe/CdS/ITO substrates (annealed CdS/CdTe heterojunctions in presence of CdCl₂).

Figure 6 The XRD patterns for CdTe thin films deposited by HWT onto CdS/ZnO:Al structures: (1) unannealed and (2) annealed in presence of CdCl₂.

Figure 7 The reflection spectra (FTIR) for as-deposited CdTe thin film onto CdS/SnO₂/Glass substrate.

Table captions

Table 1

The peak reference –measured data for 80 nm cubic CBD CdS (F43 m, AMCSD #18121) deposited onto ITO substrates

Table 2

The peak reference – measured data for hexagonal CSS CdS (P63 mc, AMCSD #15177) deposited onto ZnO:Al substrates

Table 3

Structural parameters for CdS thin films deposited on different substrates.

Table 4

The peak reference – measured data for cubic CSS CdTe deposited onto CdS/iZnO/ZnO:Al/Glass substrates (F43 m, AMCSD #11518)

Table 1[Click here to download Figures \(if any\): Table 1 VATAVU_MJB4P revised 3.doc](#)**Table 1**

The peak reference –measured data for 80 nm cubic CBD CdS (F43 m, AMCSD #18121) deposited onto ITO substrates

2Θ ($^{\circ}$)	I_{obs} (arb.units)	Index hkl	P_{hkl}
26.9	82.8	(111)	1.41
31.2	0.4	(200)	0.38
44.6	32.7	(220)	1.00
52.9	18.1	(311)	1.11
55.4	7.9	(222)	1.08

Table 2[Click here to download Figures \(if any\): Table 2 VATAVU_MJB4P revised 3.doc](#)**Table 2**

The peak reference – measured data for hexagonal CSS CdS (P63 mc, AMCSD #15177) deposited onto ZnO:Al substrates

2Θ ($^{\circ}$)	I_{obs} (arb.units)	Index hkl	P_{hkl}
24.8	0.2	100	0.12
26.5	358.3	002	5.12
28.2	0.6	101	0.21
36.6	23.3	102	1.48
43.7	1.8	110	0.22
47.9	107.0	103	3.32
50.8	1.0	200	0.30
51.8	7.4	112	0.70
52.8	0.9	201	0.27
54.6	11.0	004	0.81
58.3	3.2	202	0.38
60.9	6.4	104	0.68
66.8	15.1	203	1.10
69.2	1.4	210	0.36
72.4	4.2	114	0.50
75.5	0.6	212	0.70

Table 3

Structural parameters for CdS thin films deposited on different substrates.

Structure	CdS lattice parameter		interplanar distance, Å	Additional information / Reference
	a , Å	c , Å		
CdS _{CBD} /ITO	5.7378	-	$d_{(111)}=3.3127$	CdS Cubic ICSD 29278
CdS _{CSS} /ITO	4.1356	6.7241	$d_{(002)}=3.3620$	CdS hexagonal AMCSD 15177
CdS _{CSS} /i-ZnO/ZnO:Al	4.1471	6.7146	$d_{(002)}=3.3572$	
CdS _{CSS} /ZnO:Al	4.1439	6.7132	$d_{(002)}=3.3566$	

Table 4[Click here to download Figures \(if any\): Table 4 VATAVU_MJB4P revised 3.doc](#)**Table 4**

The peak reference – measured data for cubic CSS CdTe deposited onto CdS/iZnO/ZnO:Al/Glass substrates (F43 m, AMCSD #11518)

2Θ ($^{\circ}$)	I_{obs} (arb.units)	Index hkl	P_{hkl}
23.7	8468.968	111	5.77
27.4	4.079	200	0.10
39.2	99.506	220	0.43
46.3	279.628	311	0.85
48.5	9.102	222	0.10
56.6	148.755	400	0.63
62.3	40.956	331	0.31
64.1	3.449	420	0.06
71.0	105.821	422	0.59
76.1	170.742	333	1.07

Figure 1a

[Click here to download Figures \(if any\): Figure 1a VATAVU_MJB4P revised 3.doc](#)

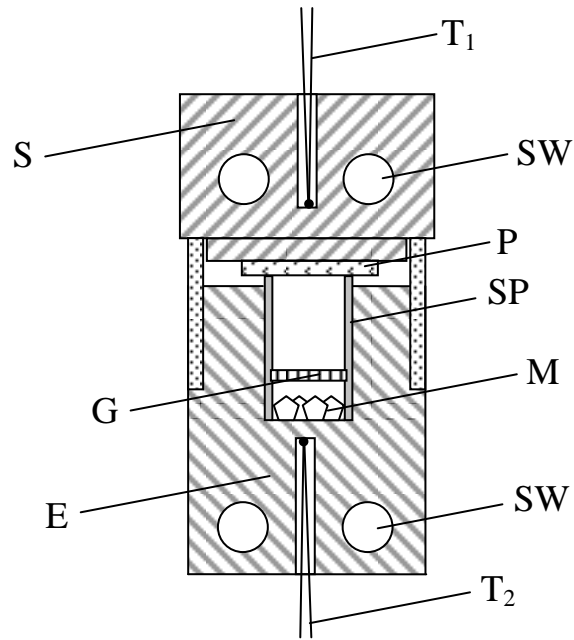


Figure 1a

Figure 1b

[Click here to download Figures \(if any\): Figure 1b VATAVU_MJB4P revised 3.doc](#)

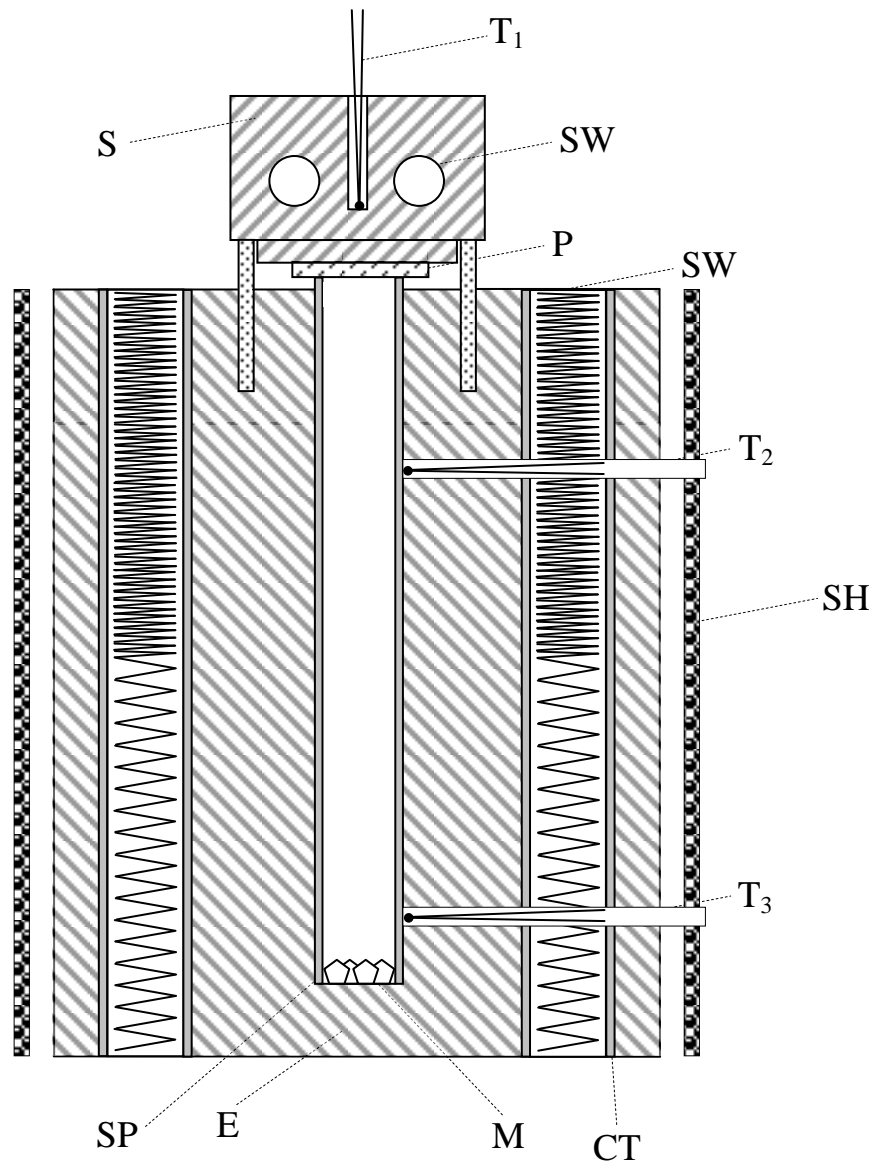


Figure 1b

Figure 2a

[Click here to download Figures \(if any\): Figure 2a VATAVU_MJB4P revised 3 TS.doc](#)

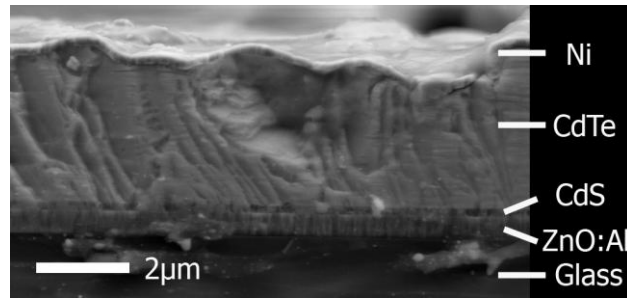


Figure 2a

Figure 2b

[Click here to download Figures \(if any\): Figure 2b VATAVU_MJB4P revised 3 TS.doc](#)

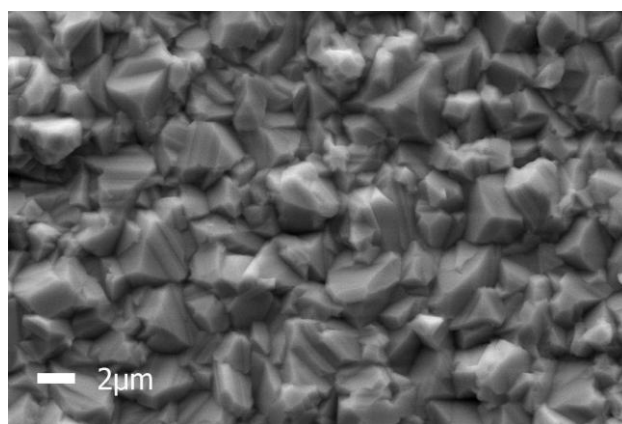


Figure 2b

Figure 3

[Click here to download Figures \(if any\): Figure 3 VATAVU_MJB4P revised 3_MR.doc](#)

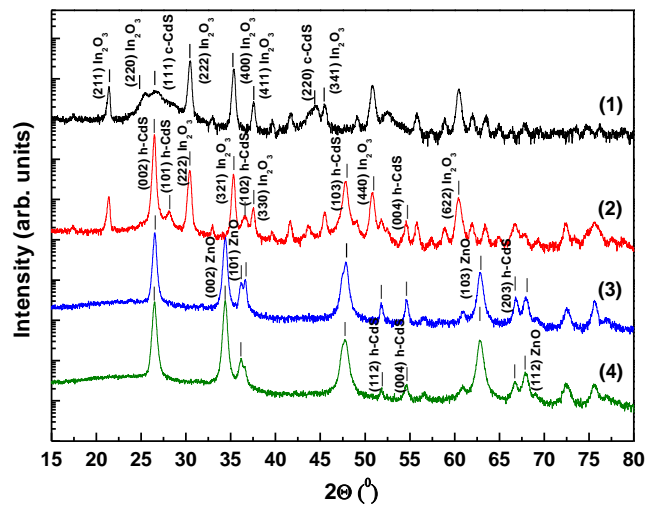


Figure 3

Figure 4

[Click here to download Figures \(if any\): Figure 4 VATAVU_MJB4P revised 3_MR.doc](#)

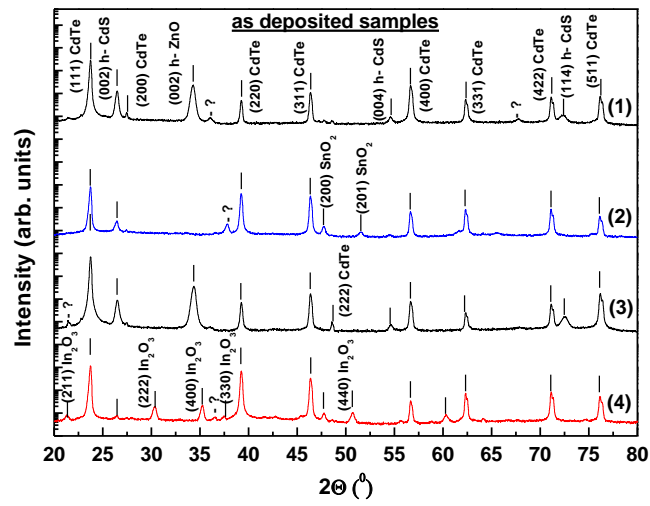


Figure 4

Figure 5

[Click here to download Figures \(if any\): Figure 5 VATAVU_MJB4P revised 3_MR.doc](#)

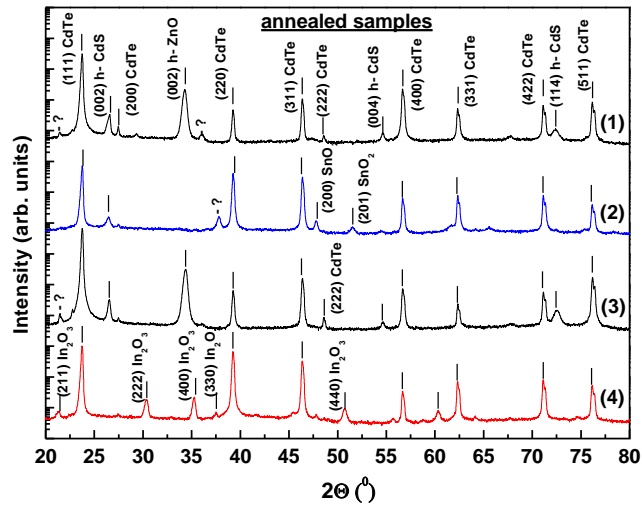


Figure 5

Figure 6

[Click here to download Figures \(if any\): Figure 6 VATAVU_MJB4P revised 3_MR.doc](#)

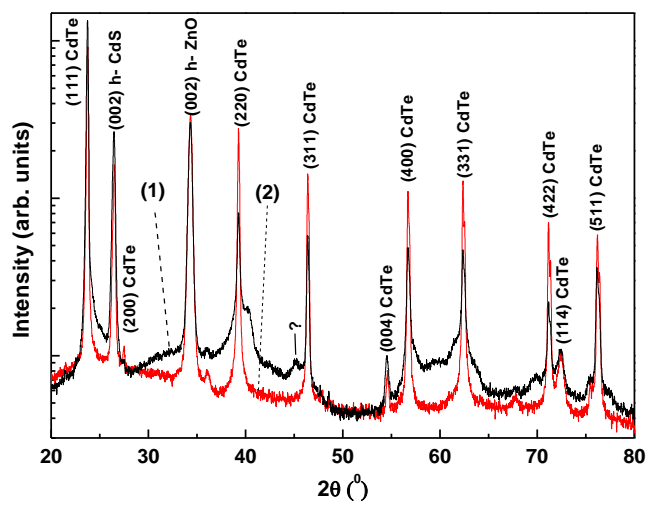


Figure 6

Figure 7

[Click here to download Figures \(if any\): Figure 7 VATAVU_MJB4P revised 3_MR.pdf](#)

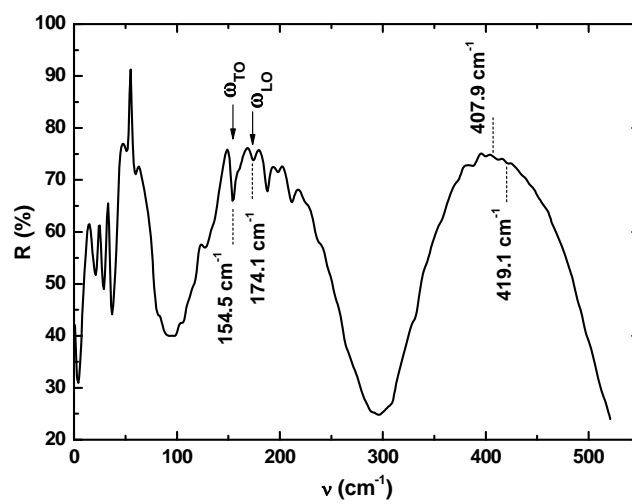


Figure 7